Article:

Perry, James M, Nagai Kanasaki, Yu, Karadakov, Peter Borislavov orcid.org/0000-0002-2673-6804 et al. (1 more author) (2021) Mechanism of dye solubilization and de-aggregation by urea. DYES AND PIGMENTS. 109530. ISSN 0143-7208

https://doi.org/10.1016/j.dyepig.2021.109530

Mechanism of dye solubilization and de-aggregation by urea

James M. Perry[1,†], Yu Nagai Kanasaki[2,†,*], Peter B. Karadakov[1], Seishi Shimizu[1,*]

[1]Department of Chemistry, University of York, Heslington, York YO10 5DD, United Kingdom.

[2]Graduate School of Humanities and Social Sciences, Hiroshima University, Japan

†Equal contribution

KEYWORDS: dye / urea / solubility / aggregation / statistical thermodynamics / water structure

Corresponding Authors:

Seishi Shimizu York Structural Biology Laboratory, Department of Chemistry, University of York, Heslington, York YO10 5DD, United Kingdom.

Tel: +44 1904 328281, Fax: +44 1904 328281, Email: seishi.shimizu@york.ac.uk

Yu Nagai Kanasaki Graduate School of Humanities and Social Sciences, Hiroshima University, Japan

Tel: +81-82-424-6852, Fax: +81-82-422-7133, Email: yukanasaki@hiroshima-u.ac.jp

ABSTRACT

Urea is an effective solubilizer for dyes with low aqueous solubility. To establish, at a molecular level, the reason behind the action of urea as an effective solubilizer, we employ a rigorous statistical thermodynamics approach based on the Kirkwood-Buff theory of solutions. We show that (i) contrary to the classical hypothesis on "water structure breaking", the effect of urea on dye hydration makes a minor contribution to solubilization; (ii) the driving force of solubilization is the accumulation of urea around hydrophobic dye molecules.

1. Introduction

Water is the most common dissolution medium for dyeing fibres [1–3]. Dye molecules need to be dispersed in solution before they are adsorbed onto or react with textile fibres [4–7]. However, their low aqueous solubility and self-aggregation make this dispersion into water problematic [8–14]. The low solubility of dyes derives from their hydrophobicity, whereas self-aggregation is attributed to their amphiphilicity [15,16].

Solubilizing agents, such as surfactants [17–23], cosolvents [24], or hydrotropes [25–27] are employed to improve aqueous dye solubility. Urea is one of the most common dye solubilizers which has been used successfully for centuries [28–32]. In addition to its ability to improve dye solubility in water [25,30], urea also enhances dye de-aggregation [33–36] and the swelling of the fibres in water [32,33,37–39]. Furthermore, low dye solubility leads to self-aggregation in water, which becomes more prominent as the concentration of the dye increases [34,40,41]. This unconducive effect in dyeing can, however, be reduced by the addition of urea, due to its propensity to enhance dye de-aggregation [34,42,43].

Much of the progress in understanding the effect of urea on dye solubility and aggregation was made decades ago, before the advent of a modern rigorous statistical thermodynamic approach to solubility. This theory has already been demonstrated to be effective in establishing the solubilization mechanisms of small solutes in the presence of cosolvents and hydrotropes [44–46].

It is therefore timely to revisit the important and classical question about the effects of urea using state-of-the-art solution theory.

The goal of this paper is to clarify the two questions: firstly, why does urea improves dye solubility and secondly, why does it enhance dye de-aggregation? The following two hypotheses for these phenomena have been proposed, examined, and debated for many years:

1. Urea changes the water structure around dye molecules.
2. Urea interacts strongly with the dye, enhancing de-aggregation.

According to the "water structure" (hypothesis 1, above) [47], the low solubility of dyes in water stems from the formation of an ice cage structure of water molecules around a dye in solution. Urea acts as a dispersing agent to change this ice cage structure [25,35,48] and breaks the hydrogen bonds between water molecules arranged around the dye [30]. However, the evidence presented for the ice cage hypothesis was aimed only to rationalize solubility enhancement [49] and did not have a rigorous statistical thermodynamics grounding.

According to the urea-water interaction (hypothesis 2, above), dispersing agents such as urea improve solubility by forming complexes with solute molecules [50,51], either via hydrogen bonding [52] between the carbonyl group of urea and a polar group on the dye or through the hydrophobic effect [37,53]. This is because hydrogen bonds between urea and dye seem to be weaker than those between water and dye [54]. However, urea is a hydrophilic molecule. Hence, both hypotheses need to be re-examined in light of the state-of-the-art statistical thermodynamics theory.

Here, we revisit the classical questions of dye solubilization and de-aggregation mechanisms by urea. We will present clear answers to these questions, by quantifying the interactions (affinities) between different solution components directly from solubility, density, and activity data from the literature. Unlike the previously published work, we are able to compare different interaction strengths, which allows quantitative examination of the validity of existing hypotheses. The convincing track record of this approach follows from its model- and assumption-free nature; the analysis uses experimental data and the principles of statistical thermodynamics only. The strengths of interactions have been quantified using statistical thermodynamics through the Kirkwood-Buff integrals (KBI) [44–46,55–58].

However, due to their large sizes, the dye molecules discussed in the present paper require special treatment which was not required in our previous work. As we will show, the dye-water and dye-urea KBIs are both large and negative; the positive contributions from the accumulation of urea or water around a dye are overridden by a large, negative contribution from excluded volume due to the large molecular sizes of the dyes [44–46,55–58]. Therefore, the excluded volume effect must be separated from the solvent accumulation effect to achieve clear pictures of the solubilization and de-aggregation mechanisms.

2. Theory

2.1. Driving forces of solubilization

Let us consider a solution consisting of the following components: solute (denoted as u), water (1) and cosolvent (2). For this three-component system (with dilute solute), we have previously shown [45,59,60] that the Kirkwood-Buff integrals (KBIs) quantify both the specific and non-specific interactions between solution components can be determined solely from a combination of experimental data via statistical thermodynamics. Figure 1 illustrates the meaning of solute-water and solute-urea KBIs, G_{u1} and G_{u2} [45,59,60], i.e., the increments of water and urea concentrations around the solute molecule compared to the bulk solution. Figure 1 shows that KBIs are essentially the increments per molar concentration of the species.

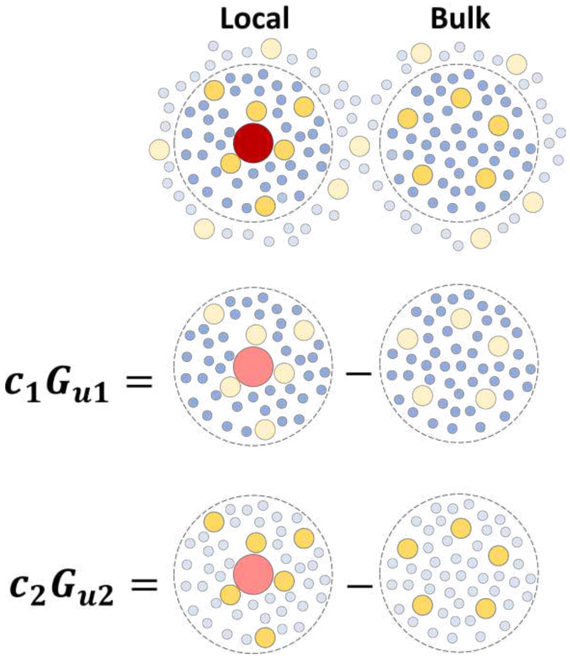

Figure 1: A schematic representation of the local (a) and bulk (b) concentrations and their difference. Urea (yellow) are concentrated around the dyes (red) in the local area ((a)) compared to the bulk ((b)). The difference between local-bulk concentration is calculated as ΔG_{ui}.

Solubility measurements report the dependence of dye solubility, s_u, on the molar concentration of cosolvent, c_2. Our aim is twofold: to understand the molecular basis of such dependence in terms of interactions between different species, and to identify the dominant contribution. To do so, solubilization can be expressed in terms of KBIs [44–46] as:

$$\frac{1}{s_u}\left(\frac{\partial s_u}{\partial c_2}\right)_{T,P} = \left(\frac{\partial \ln s_u}{\partial c_2}\right)_{T,P} = \frac{G_{u2}-G_{u1}}{1+c_2(G_{22}-G_{21})} \quad (1)$$

Eq. (1) identifies the following two contributions to solubilization:

1. $G_{u2} - G_{u1}$, the **preferential affinity** between a dye and a cosolvent over that between a dye and water, increasing the solubility.
2. $1 + c_2(G_{22} - G_{21})$, the **preferential self-association of cosolvents**, driven by cosolvent-cosolvent affinity (G_{22}) over affinity between cosolvent and water (G_{21}), which reduces the solubilization [49].

In order to elucidate the mechanism of solubilization, these two contributions, as well as all the underlying KBIs, should be quantified. In our previous papers on the solubilization of small molecules by hydrotropes, factor 1 was shown to be dominant whereas factor 2 was found to be the secondary, more minor contribution [44–46,55,58].

2.2. Solvation shell contribution to the Kirkwood-Buff integrals

The large sizes and, consequently, large molar volumes of the dye molecules lead to large and negative G_{u2} and G_{u1} values, following from the contribution of the large excluded volume (V_E) of the solute molecules to both KBIs. Yet, it is the structure of the aqueous solution around the dye that was the focus of the debate on the mechanism of dye solubilization. This contribution (hereafter referred to as the solvation shell contribution) should be extracted from experimental data by subtracting out the excluded volume contribution. This can be achieved by introducing the following solvation-shell contributions to KBIs [59],

$$G'_{ui} = G_{ui} + V_E \tag{2}$$

How can G'_{u2} and G'_{u1} be determined from experimental data? To answer this question, let us start from the well-known relationships involving these KBIs [59,60]:

(a) The dependency of dye solubility, s_u , on water activity a_1

$$-\left(\frac{\partial \ln s_u}{\partial \ln a_1}\right)_{T,P;c_u \to 0} = c_1(G_{u2} - G_{u1}) \tag{3}$$

where c_i is the molar concentration of the component i . Here, $G_{u2} - G_{u1}$ represents the preferential solvation of the cosolvent relative to water, which is very much a competition between cosolvent-solute and cosolvent-water affinities [59,60].

(b) Partial molar volume of the solute, V_u

$$V_u = -c_1V_1G_{u1} - c_2V_2G_{u2} + RT\kappa_T \tag{4}$$

where V_1 and V_2 are the partial molar volumes of water and cosolvent, and κ_T is the isothermal compressibility of the bulk solution, whose contribution to V_u (namely $RT\kappa_T$) is ca. 1.2 cm^3 mol^{-1} at 298 K, hence it is negligible [59,60].

Eqs. (3) and (4) can be expressed in terms of G'_{u1} and G'_{u2} in the following straightforward manner:

$$-\left(\frac{\partial \ln s_u}{\partial \ln a_1}\right)_{T,P;c_u \to 0} = c_1(G'_{u2} - G'_{u1}) \tag{5}$$

$$V'_u = V_u - V_E = -c_1V_1G'_{u1} - c_2V_2G'_{u2} \tag{6}$$

Eqs. (3)-(6) in combination will be used as the foundation of our analysis.

Note that the same V_E was used in Eq. (2) for calculating G'_{u1} and G'_{u2} [59,61]. By doing so, the solvation shell relationships, Eqs. (5) and (6), retain the same mathematical form as the original KBIs, Eqs. (3) and (4). In this way, the preferential affinity, $G_{u2} - G_{u1}$, can be attributed solely to solvation shell contributions, because $G'_{u2} - G'_{u1} = G_{u2} - G_{u1}$ under the transformation via Eq. (2). For V_E, we will adopt Chalikian's estimation [62] of the volume around a solute inaccessible to water. Under this definition, the size difference between water and cosolvent is reflected in G'_{u2}; for example, a cosolvent larger in molecular size than water has a negative contribution to G'_{u2} from the excluded volume effect [59,61].

2.3. A simple criterion to identify the origin of preferential solvation

Preferential solvation, as shown above, is defined in terms of competitive affinity. Is preferential solvation mainly due to solute-cosolvent affinity, or to solute hydration? Does the cosolvent-induced change of solute hydration play a dominant role? Having introduced solvation shell KBIs, we can answer these questions. The first step is to solve the simultaneous equations (Eqs. (3) and (6)), which yield:

$$G_{u1} = -V_u + V_2 \frac{c_2}{c_1} \left(\frac{\partial \ln s_u}{\partial \ln a_1} \right)_{T,P;c_u \to 0} \tag{7a}$$

$$G_{u2} = -V_1 \left(\frac{\partial \ln s_u}{\partial \ln a_1} \right)_{T,P;c_u \to 0} - V_u \tag{7b}$$

$$G'_{u1} = -V'_u + V_2 \frac{c_2}{c_1} \left(\frac{\partial \ln s_u}{\partial \ln a_1} \right)_{T,P;c_u \to 0} \tag{8a}$$

$$G'_{u2} = -V_1 \left(\frac{\partial \ln s_u}{\partial \ln a_1} \right)_{T,P;c_u \to 0} - V_u^{\prime} \tag{8b}$$

Note that the difference between the solute-water and solute-urea KBIs can be observed in how the solubility and volumetric data have been combined. Useful insights can be drawn from Eqs. (7) and (8), which will be discussed using the experimental data.

2.4. Dye dimerization

Dye aggregation occurs in a stepwise manner (i.e. monomer → dimer → trimer, etc.) and can eventually result in the formation of a colloidal-sized aggregate [1]. This paper focuses on the dimerization process as the initial step, for which experimental dimerization constants are available in the literature.

The main advantage of a general and assumption-free theory, presented in Sections 2.1-2.3, is in its ability to account for different phenomena using the same set of equations. The equations defining solubilization can be adapted easily to quantify dye aggregation with the following modifications only:

- the dimerization constant K_a replaces the solubility s_u;
- KBI changes upon dimerization ΔG_{ui} are used instead of the KBIs themselves, G_{ui};
- ΔG_{ui} is used instead of $\Delta G'_{ui}$, because dimerization does not affect the van der Waals volume.

As in the previous study [63], the change of KBIs accompanying caffeine dimerization was defined as $\Delta G_{ui} \equiv G_{ui}^{(d)} - 2G_{ui}^{(m)}$, where $G_{ui}^{(d)}$ and $G_{ui}^{(m)}$ represent the KBI difference between solute dimer and species i, and solute monomer and species i, respectively. Using these quantities, the water activity dependence of the dimerization constant K_a can be expressed in terms of the KBI difference as

$$-\left(\frac{\partial \ln K_a}{\partial \ln a_1}\right)_{T,P;c_u \to 0} = c_1(\Delta G_{u2} - \Delta G_{u1}) \tag{9}$$

In addition, the volume change upon dimerization ΔV_u can also be expressed using the same pair of KBIs as

$$\Delta V_u = -c_1 V_1 \Delta G_{u1} - c_2 V_2 \Delta G_{u2} \tag{10}$$

Hence, solving Eqs. (9) and (10) yields

$$\Delta G_{u1} = -\Delta V_u + V_2 \frac{c_2}{c_1}\left(\frac{\partial \ln K_a}{\partial \ln a_1}\right)_{T,P;c_u \to 0} \tag{11}$$

$$\Delta G_{u2} = -V_1 \left(\frac{\partial \ln K_a}{\partial \ln a_1}\right)_{T,P;c_u \to 0} - \Delta V_u \tag{12}$$

Eqs. (11) and (12) will be useful in identifying the cause of the urea-induced dissociation of dye dimers.

3. Sources and analysis of experimental data

3.1. Choice of experimental data for dye solubilization

To understand how urea increases the solubility of dyes from a molecular perspective, KBIs have to be calculated for the dye-water and dye-urea interactions (Eq. (7a) and (7b)). To this end, experimental data on dye solubility, osmotic coefficient, and density are required.

We have chosen the systematic dye solubility data published by Takagishi et al. [31] and Katayama et al. [49] on a series of biphenyl dyes, whose chemical structures are shown in Table

1. Osmotic coefficient data for the aqueous solution of urea have been taken from Stokes [64]. Density data for urea in aqueous solution have been taken from Kawahara et al. [65].

3.2. Analysis of experimental data for dye solubilization

As a first step towards calculating the dye-urea preferential affinity from solubility data using Eq (3), we need to investigate how the expression $-RT\ln\frac{s_u}{s_u^0}$ (where s_u is the molar solubility in aqueous urea solution and s_u^0 is that in pure water) depends on urea concentration (c_2). The experimental data reported in the literature [30,49] refers to x_u/x_u^0, a corresponding mole fraction ratio. This can be converted to $\frac{s_u}{s_u^0}$ via $\frac{s_u}{s_u^0}=\frac{x_u}{x_u^0}\frac{c_1+c_2}{c_1^0}$, where c_i is the molar concentration of the species i. To calculate dye-urea preferential affinity, $\ln\frac{s_u}{s_u^0}$ has to be plotted against $-\ln a_1$, as shown in Figure 2(b).

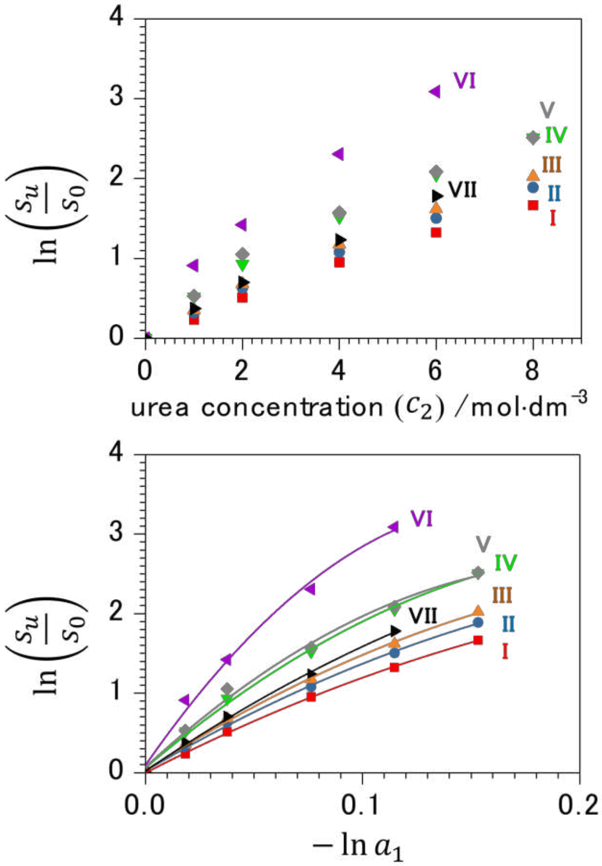

Figure 2: Dependence of dye solubility on (a) urea concentration and (b) $-\ln a_1$ (where a_1 is the activity of water and the relationship shows preferential urea–dye interaction (eq (5)). The solubility data have been taken from Ref [49].

Here water activity, a_1, was calculated using the osmotic coefficient of urea in aqueous solutions[64]. To calculate the derivative $-\left(\frac{\partial \ln s_u}{\partial \ln a_1}\right)_{T,P,n_u \to 0}$ in Eq. (7), polynomial regression analysis was performed, as summarised in Table 2. The partial molar volume of the dye, V_u, in Eq. (4) was calculated using the group additivity scheme proposed by Lepori and Gianni [66], as summarised in Table 3.

3.3. Dye dimerization

Experimental data for the dye dimerization study in aqueous urea solution were selected from the literature. The chemical structures of these dyes are summarized in Table 4. To calculate the KBIs, ΔG_{u1} and ΔG_{u2} via Eqs. (11) and (12), the following quantities need to be calculated: $V_1 \left(\frac{\partial \ln K_a}{\partial \ln a_1}\right)_{T,P;c_u \to 0}$ and $\Delta V_u \frac{c_2}{c_1} \left(\frac{\partial \ln K_a}{\partial \ln a_1}\right)_{T,P;c_u \to 0}$. $\Delta V_u \frac{c_2}{c_1} \left(\frac{\partial \ln K_a}{\partial \ln a_1}\right)_{T,P;c_u \to 0}$ is negligibly small because c_2 is small.

The experimental data of K_a for both Leuco and Fluoran type dyes have been taken from the literature [42,43]. Due to the scarcity of published data, $\frac{\partial \ln K_a}{\partial \ln a_1}$ was calculated approximately from K_a values for 0 M and 1 M urea, as summarised in Table 5.

3.4. Calculation of excluded volume

Solvation shell KBIs were calculated from the dyes excluded volumes. To calculate excluded volumes, the gas-phase geometries of azobenzene (I), biphenyl (II), 4-aminoazobenzene (III), methyl yellow ((*E*)-*N*,*N*-dimethyl-4-(phenyldiazenyl)aniline, IV), (*E*)-2,2'-((4-(phenyldiazenyl)phenyl)azanediyl)bis(ethan-1-ol) (V), α-naphthyl red ((*E*)-4-(phenyldiazenyl)naphthalen-1-amine, VI), solvent yellow 7 ((*E*)-4-(phenyldiazenyl)phenol, VII), methylene blue (3,7-bis(dimethylamino)phenothiazin-5-ium chloride, VIII) and rhodamine B ([9-(2-carboxyphenyl)-6-diethylamino-3-xanthenylidene]-diethylammonium chloride, IX) were optimized using density functional theory (DFT), at the B3LYP-D3(BJ)/def2-SVP level (B3LYP with Grimme's D3 empirical dispersion corrections and Becke-Johnson damping, within the standard def2-SVP basis set). Each optimized geometry was confirmed as a local minimum through diagonalization of the respective analytic nuclear Hessian. All of these calculations were carried out using GAUSSIAN16 [67]. For each species, the excluded volume was calculated as the volume within the Connolly surface [68] for a probe radius of 1.4 Å, using Connolly's Molecular Surface Package version 3.9.2. DFT optimized geometries and computational data can be found in the Electronic Supporting Information.

4. Results and Discussion

4.1. Effect of urea on dye solubilization

The positive sign of the partial derivative $-\left(\frac{\partial \ln s_u}{\partial \ln a_1}\right)_{T,P,n_u\to 0}$ is similar to that observed in previous work on the solubility of small solutes in the presence of urea [45] (Figure 4). According to Eq. (3), this means that the positive preferential affinity, $G_{u2} - G_{u1}$, contributes to the urea-induced increase of solubility (Figure 3). The contribution from urea self-association in water, $1 + c_2(G_{22} - G_{21})$, is observed in Figure 3 to show next to no deviation from the value of 1, which is also in agreement with previous work [45], and indicates that this contribution is negligible in comparison to $G_{u2} - G_{u1}$.

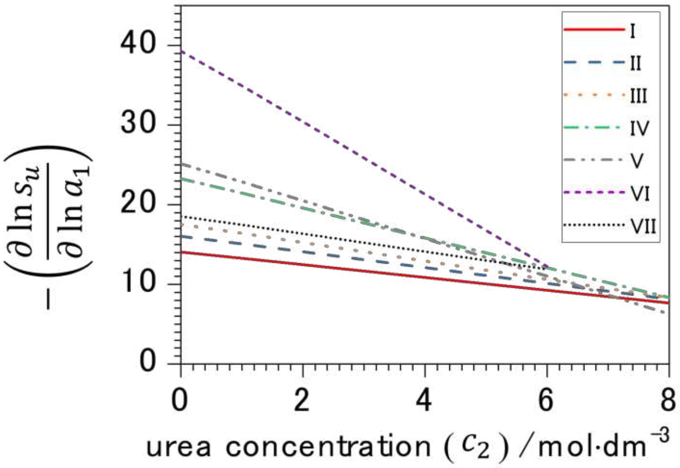

Figure 3: Plots of $-\left(\frac{\partial \ln s_u}{\partial \ln a_1}\right)$ for the dye against urea concentration. The relationship shows the difference between the KB parameters for urea-dye (G_{u2}) and water–dye (G_{u1}) calculated using eq (3).

Having identified the difference $G_{u2} - G_{u1}$ as the driving force for solubilization, the most important question now is whether the dye-urea or dye-water interaction is dominant in $G_{u2} - G_{u1}$. Ultimately, the question as to whether the dye-urea interaction hypothesis or the water structure hypothesis provides the correct explanation for dye solubilization in urea (see Section 1) can now be answered.

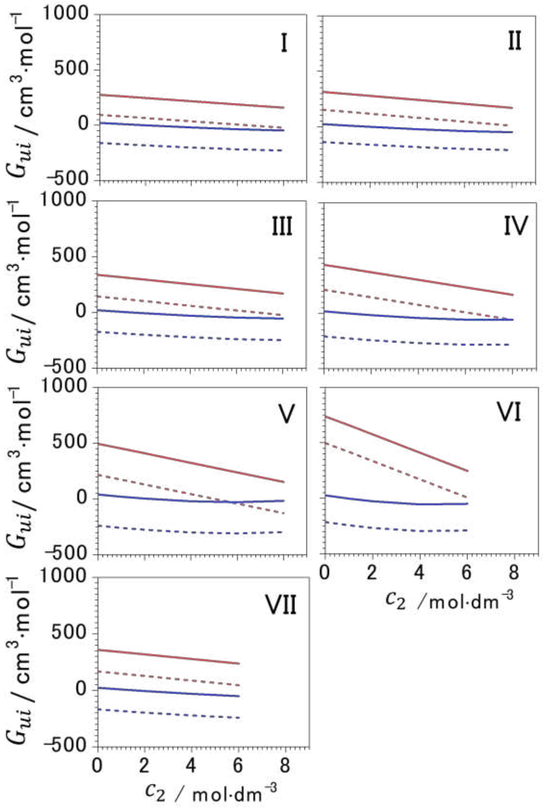

Figure 4: Independent determination of urea-dye and water-dye KB parameters. G_{u1} (blue dashed line) and G_{u2} (red dashed line) were corrected to G'_{u1}(blue solid lines) and G'_{u2} (red solid lines).

Figure 4 shows that G_{u1} and G_{u2} have opposite signs and neither can be negligibly small when these are compared to one another. However, due to the large molecular sizes of the dyes, the excluded volume effect must be accounted for. This is achieved by subtraction of the same excluded volume contributions to G_{u1} and G_{u2} to calculate the solvation-shell contributions to the KBIs (Eq. (2)), namely, G'_{u1} and G'_{u2}.

Figure 4 also shows that G'_{u2} is much larger than G'_{u1} for all dyes. We can therefore conclude that the dye-urea interaction G'_{u2} is the dominant contribution which drives the urea-induced solubilization of dyes. The minor contribution from the dye-water interaction, G'_{u1}, shows that the urea-induced change of dye hydration contributes very little to solubilization. Our analysis, based on a rigorous statistical thermodynamics theory, supports the dye-urea interaction hypothesis but does not support the water structure hypothesis.

4.2. The order-of-magnitude analysis supports the dominance of the dye-urea interaction

Here we show that the same conclusion regarding the relative magnitudes of G'_{u1} and G'_{u2} , as in Section 4.1, can be reached simply via an order-of-magnitude analysis. We will discuss two conditions: at (i) low urea concentration and (ii) a few molars of urea.

(i) At $c_2 \to 0$ limit. Eqs. (8a) and (8b) at this limit become:

$$G'_{u1} \simeq -V'_u \tag{13}$$

$$G'_{u2} \simeq -V_1 \left(\frac{\partial \ln s_u}{\partial \ln a_1}\right)_{T,P;c_u \to 0} - V'_u \tag{14}$$

A comparison of $-V_1 \left(\frac{\partial \ln s_u}{\partial \ln a_1}\right)_{T,P;c_u \to 0}$ (254.3 to 711.0 cm^3 mol^{-1}, using $\left(\frac{\partial \ln s_u}{\partial \ln a_1}\right)_{T,P;c_u \to 0}$ from Figure 3) and V'_u (18.0 to 39.8 cm^3 mol^1 Table 3) shows that the contribution from G'_{u2} is dominant over that of G'_{u1}. The effect of urea on dye hydration can thus be neglected.

(ii) **At a few molars of c_2**. This is the situation in which solubilization takes place. When the second term in Eq. (8a) becomes dominant,

$$G'_{u1} \simeq V_2 \frac{c_2}{c_1} \left(\frac{\partial \ln s_u}{\partial \ln a_1}\right)_{T,P;c_u \to 0} \tag{15}$$

$$G'_{u2} \simeq -V_1 \left(\frac{\partial \ln s_u}{\partial \ln a_1}\right)_{T,P;c_u \to 0} \tag{16}$$

Eq. (15) already shows that the dye hydration contribution V'_u is negligible as a contribution to G'_{u1}. The relative magnitude of G'_{u2} over G'_{u1} can be calculated simply via the ratio between them:

$$\frac{G'_{u1}}{G'_{u2}} = -\frac{V_2}{V_1}\frac{c_2}{c_1} \tag{17}$$

The dominant contributor to the above ratio is $\frac{c_2}{c_1}$, which, at 3 M is about 0.05, and increases to around 0.1 at 6M. $\frac{V_2}{V_1}$ has a value of approximately 2, hence showing that urea cannot override such a small magnitude of $\frac{c_2}{c_1}$. We observe, therefore, that the contribution of G'_{u1} is minor compared to that of G'_{u2}.

Thus, the order-of-magnitude analyses for both cases show that our conclusion about the dominance of G'_{u2} over G'_{u1} is a robust one. The dye-water interaction (G'_{u1}) is negligibly small compared to dye-urea interaction over the whole urea concentration range (1-8 M) studied here. Thus, the order-of-magnitude analysis confirms our conclusion that the breaking of the water structure by urea cannot explain the solubilization of dyes by urea.

4.3. The effect of urea on dye dimerization

The presence of urea weakens dye aggregation because of a negative $\Delta G_{u2} - \Delta G_{u1}$, as seen from Eq. (9). To establish which of the two KBI differences (dye-water or dye-urea) is responsible for de-aggregation, in Table 5 we report the values of $V_1 \left(\frac{\partial \ln K_a}{\partial \ln a_1}\right)_{T,P;c_u \to 0}$ and $-\Delta V_u$ which are the first and the second terms in Eq. (12). Here, ΔV_u has been taken from the literature [69,70]. For both dyes $V_1 \left(\frac{\partial \ln K_a}{\partial \ln a_1}\right)_{T,P;c_u \to 0}$ is much larger in magnitude than $-\Delta V_u$. Since ΔG_{u1} is dominated by $-\Delta V_u$ at low urea concentrations, as seen in Eq. (11), we can conclude that ΔG_{u2} makes the dominant contribution to urea-induced dye de-aggregation. The signs of ΔG_{u2} inferred from Eqs. (12) and Table 5 are negative, showing that the urea-dimer interaction is weaker than the interaction between urea and the two monomers, which can be rationalized by the suggestion that the reduction of surface area upon dye dimerization leads to weaker interaction with urea. Thus, the dominant contribution from ΔG_{u2} shows that the reduction of the urea-dye interaction that accompanies dimerization is the cause of dye de-aggregation by urea.

Our statistical thermodynamics analysis confirms, yet again, that dye de-aggregation by urea is due to the dye-urea interaction rather than to the change of dye hydration in the presence of urea.

4.4. Solubilization mechanism

The strength of our approach is in its capacity to quantify the driving forces of solubilization directly from experimental data based directly on the principles of statistical thermodynamics. The fundamental relationships for solubilization and aggregation (Eqs. (3)-(12)) were derived without any approximations or model assumptions [44,45,55,71]. Such an approach may seem at odds with the more common theoretical approaches to solubilization, such as simple models and computer simulations. The Hansen solubility parameters (HSP) [72] or COSMO-RS [73] are the most commonly used simple solvation models, yet their applicability to water and aqueous solutions are limited [74]. Force field parameterization is a prerequisite for molecular dynamics or Monte Carlo simulations, yet the force fields for the most common cosolvent, including urea, are still a matter of active research [75,76]. In contrast, Eqs. (3)-(12) do not involve any model assumptions, they are not subject to experimental verifications in the same way as for simple models or force fields. Thus, our approach, based solely on the principles of statistical thermodynamics, is advantageous in its ability to identify and quantify the contributions to solubility directly from experimental data.

Here we compare our conclusion on the mechanism of dye solubilization and de-aggregation by urea to a wider range of solubilization data. The scale of such a comparison is somewhat limited by the lack of systematic, consistent, and high-quality experimental data covering not only solubility but also activity coefficients, densities, and partial molar volumes [71]. Nevertheless, one of us has carried out an extensive literature survey on aqueous solubilization by cosolvents, hydrotropes, and surfactants, cross-correlated, whenever necessary, with density and activity data. The density and activity data were available for nicotinamide, sodium benzoate, sodium salicylate, sodium cumene sulfonate, and urea as hydrotropes [44–46,55,74]. For the solutes, solubility data were available for p-aminobenzoic acid, butyl acetate, butyl stearate, butyl acetate, benzyl benzoate, ethylbenzene, lauric acid, methyl benzoate, and o-Hydroxyacetophenone [44–46,55,74]. The solubilization mechanism calculated from the above dataset is consistent with the present paper: solubilization is driven predominantly by a strong solute-hydrotrope affinity, while the self-association of the solubilizing agent reduces solubilization efficiency [46,74]. The reduction in solubilization efficiency becomes more prominent for hydrotropes with a stronger tendency to self-associate, such as nicotinamide, yet the dominance of solute-hydrotrope affinity remains valid [46,74].

The same solubilization mechanism applies to surfactants whose tendency for self-aggregation is stronger than hydrotropes [77]. Nevertheless, the strong solubilization capacity of surfactants has also been attributed to solute-surfactant affinity; inefficiency from surfactant self-association has been estimated to be small, contrary to the classical hypotheses [56,58,77]. Moreover, extensive literature data on solubilization in supercritical CO_2 by "entrainers" (including methanol, ethanol, n-propanol, acetone, ethyl acetate, hexane, ethylene glycol, DMF and water) has been compiled and analyzed [78,79]; the solutes in the dataset contained some dyes, including Disperse Blue 56, Disperse Orange 3, Disperse Orange 79, Disperse Violet 1, and Disperse Yellow 54 as dyes [78,79]. In contrast to the classical hypotheses on the solubilization mechanism, based on the entrainer's role in cluster formation, heterogeneity, or density increase [78,79], the calculation of KBIs has shown that the entrainers work predominantly by entrainer-solute affinity via hydrogen bonding [78,79], which is consistent with our present study.

Thus, a strong affinity between solute and solubilizing agent (cosolvents, surfactants, hydrotropes, or entrainers) seems to be the driving force of solubilization, while the aggregation of the solubilizing agent in bulk plays a secondary (often minor) role [44–46,55,58,71,74,77–79]. This conclusion from rigorous statistical thermodynamics was underscored further by a direct observation using ^{1}H-NMR [80].

We expect that further thermodynamic measurements not only of solubility but also of the osmotic and volumetric properties in combination will be undertaken. We have already provided a series of web-based tools that can calculate KBIs automatically and interactively straight from experimental measurements [46,74,78,79].

5. Conclusion

Dye solubilization is influenced strongly by the presence of urea. Whether this is due to the effect of urea on water structure and dye hydration or urea-dye interaction has been debated for decades without reaching a decisive conclusion. We have revisited this classical question via state-of-the-art statistical thermodynamics theory.

The advantage of our approach is in its ability to quantify interactions between molecular species based on molecular distributions using Kirkwood-Buff integrals. These interactions can be calculated from experimental data alone. The recent track record of this approach in clarifying the role of cosolvents on solvation and macromolecular conformational equilibria prompted revisiting this classical question in dye solubilization.

We have shown that, for both dye solubilization and de-aggregation, dye-urea interaction plays a dominant role, and dye-water interaction makes a negligibly small contribution. Due to the large molecular size of dyes, we have separated the contributions from the excluded volume effect and solvent distribution around a dye. Our conclusion was confirmed further by an order-of-magnitude analysis and is demonstrated to be robust, despite an approximate estimation of the excluded volume effect. This approach, based solely on the principles of statistical thermodynamics, is readily applicable to any solubilizers, any solvents and any dyes.

Acknowledgements

This work was supported by JSPS KAKENHI Grant-in-Aid for Young Scientists (Grant Number K1813030).

References

[1] Burkinshaw SM. Physico-Chemical Aspects of Textile Coloration. Chichester: Wiley; 2015. https://doi.org/10.1002/9781118725658.

[2] Blackburn R. Sustainability challenges of the textiles, dyeing and finishing industries: opportunities for innovation. ACS Webinar 2015:1–32.

[3] Kant R. Textile dyeing industry an environmental hazard. Nat Sci 2012;04:22–6. https://doi.org/10.4236/ns.2012.41004.

[4] Bird CL. The dyeing of acetate rayon with disperse dyes. I. Aqueous solubility and the influence of dispersed agents, II. The relation between aqueous solubility and dyeing properties. J Soc Dye Colour 1954;7:68–77. https://doi.org/10.1111/j.1478-4408.1955.tb02057.x.

[5] Bird CL, Rhyner P. The dyeing of cellulose acetate with disperse dyes. VI. Affinities, heats of dyeing and heats of Solution. J Soc Dye Colour 1957;77:199–202. https://doi.org/10.1111/j.1478-4408.1961.tb02399.x.

[6] Vickerstaff T, Waters E. The dyeing of cellulose acetate rayon with dispersed dyes. J Soc Dye Colour 1942;58:116–25. https://doi.org/10.1111/j.1478-4408.1942.tb02180.x.

[7] Bird CL, Manchester F, Harris P. Theoretical aspects of the dyeing of cellulose acetate

rayon. Discuss Faraday Soc 1954;16:85–92. https://doi.org/10.1039/DF9541600085.

[8] Patterson D, Sheldon RP. The solubilities and heats of solution of disperse dyes in water. J Soc Dye Colour 1960;76:178–81. https://doi.org/10.1111/j.1478-4408.1960.tb02369.x.

[9] Giles CH, McKay RB. The lightfastness of dyes: A review. Text Res J 1963;33:528–77. https://doi.org/10.1177/004051756303300707.

[10] Green HS, Jones F. Vapour pressures, heats of sublimation and degrees of association of some azo compounds in the vapour phase. Trans Faraday Soc 1967;63:1612–9. https://doi.org/10.1039/tf9676301612.

[11] Kuroiwa S, Ogasawara S. Solubilities of disperse dyes in water. Nippon Kagaku Kaishi 1973;9:1738–43. https://doi.org/https://doi.org/10.1246/nikkashi.1973.1738.

[12] Shibusawa T, Ohya Y, Hainayose T. Therinodynainic studies on the solution processes of disperse dyes in water. Nippon Kagaku Kaishi 1977;1977:1536–42. https://doi.org/10.1246/nikkashi.1977.1536.

[13] Hamada K, Iijima T, Amiya S. Aggregation of azo dyes containing pentafluoroaniline as a diazo component in aqueous solutions. J Phys Chem 1990;94:3766–9. https://doi.org/10.1021/j100372a076.

[14] Iyer SRS, Singh GS. Aggregation of anionic dyes in aqueous solutions. J Soc Dye Colour 1973;89:128–32. https://doi.org/10.1111/j.1478-4408.1973.tb03138.x.

[15] Clark RJH, Cooksey CJ, Daniels MAM, Withnall R. Indigo, woad, and tyrian purple: Important vat dyes from antiquity to the present. Endeavour 1993;17:191–9. https://doi.org/10.1016/0160-9327(93)90062-8.

[16] Kōyama U. Versuche der Färbung von Ölen und Fetten mit alkohollöslichen Farbstoffen. Arch Histol Jpn 1950;1:385–9. https://doi.org/10.1679/aohc1950.1.385.

[17] Takagishi T, Katayama A, Konishi K, Kuroki N. The solubility of disperse dyes in an aqueous sodium dodecyl sulfate solution. Kolloid-Z Z Polym 1969;232:689–93. https://doi.org/10.1007/BF01500165.

[18] Tehrani-Bagha AR, Holmberg K. Solubilization of hydrophobic dyes in surfactant solutions. Materials (Basel) 2013;6:580–608. https://doi.org/10.3390/ma6020580.

[19] Garcia MED, Sanz-Medel A. Dye-surfactant interactions: a review. Talanta 1986;33:255–64. https://doi.org/10.1016/0039-9140(86)80060-1.

[20] Tehrani Bagha AR, Bahrami H, Movassagh B, Arami M, Menger FM. Interactions of gemini cationic surfactants with anionic azo dyes and their inhibited effects on dyeability of cotton fabric. Dye Pigment 2007;72:331–8. https://doi.org/10.1016/j.dyepig.2005.09.011.

[21] Gokturk S, Tuncay M. Dye-surfactant interaction in the premicellar region. J Surfactants Deterg 2003;6:325–30. https://doi.org/10.1007/s11743-003-0277-y.

[22] Schramm LL, Stasiuk EN, Marangoni DG. Surfactants and their applications. Annu Reports Prog Chem - Sect C 2003;99:3–48. https://doi.org/10.1039/B208499F.

[23] Naeem K, Shah SS, Shah SWH, Laghari GM. Solubilization of cationic hemicyanine dyes in anionic surfactant micelles: A partitioning study. Monatsh Chem 2000;131:761–7. https://doi.org/10.1007/s007060050023.

[24] Takagishi T, Katayama A, Matsuoka M, Konishi K, Kuroki N. Effects of alcohols on the aqueous solubility of disperse dyes. Kolloid-Z Z Polym 1969;232:699–703. https://doi.org/https://doi.org/10.1007/BF01500167.

[25] Katayama A, Takagishi T, Konishi K, Kuroki N. Effect of sulphonic acid on the aqueous solubility of disperse dyes. Kolloid-Z Z Polym 1965;206:162–6.

https://doi.org/10.1007/BF01500234.

[26] da Silva RC, Spitzer M, da Silva LHM, Loh W. Investigations on the mechanism of aqueous solubility increase caused by some hydrotropes. Thermochim Acta 1999;328:161–7. https://doi.org/10.1016/S0040-6031(98)00637-6.

[27] Moity L, Shi Y, Molinier V, Dayoub W, Lemaire M, Aubry JM. Hydrotropic properties of alkyl and aryl glycerol monoethers. J Phys Chem B 2013;117:9262–72. https://doi.org/10.1021/jp403347u.

[28] Lagercrantz O. Papyrus Graecus Holmiensis. Uppsala: A.-B. Akademiska Bokhandeln; 1913.

[29] Datyner A, Pailthorpe MT. A study of dyestuff aggregation. Part III. The effect of levelling agents on the aggregation of some anionic dyes. Dye Pigment 1987;8:253–63. https://doi.org/10.1016/0143-7208(87)85016-7.

[30] Kissa E. Urea in reactive dyeing. Text Res J 1969;39:734–41. https://doi.org/10.1177/004051756903900805.

[31] Takagishi T, Katayama A, Kuroki N. Effects of ureas and formamides on the aqueous solubility of disperse dyes. J Chem Inf Model 1969;25:381–6. https://doi.org/10.1017/CBO9781107415324.004.

[32] Brady PR. The effect of urea on wool fibres. J Soc Dye Colour 1976;92:56–8. https://doi.org/10.1111/j.1478-4408.1976.tb03275.x.

[33] Asquith RS, Booth MAK. A study of the dyeing of wool from long liquors in the cold. J Soc Dye Colour 1970;86:393–8. https://doi.org/10.1111/j.1478-4408.1970.tb02964.x.

[34] Mukerjee P, Ghosh AK. The effect of urea on methylene blue, its self-association, and interaction with polyelectrolytes in aqueous solution. J Phys Chem 1963;67:193–7.

https://doi.org/10.1021/j100795a047.

[35] Patil K, Pawar R, Talap P. Self-aggregation of methylene blue in aqueous medium and aqueous solutions of Bu4NBr and urea. Phys Chem Chem Phys 2000;2:4313–7. https://doi.org/10.1039/b005370h.

[36] Hamlin JD, Phillips DAS, Whiting A. UV/visible spectroscopic studies of the effects of common salt and urea upon reactive dye solutions. Dye Pigment 1999;41:137–42. https://doi.org/10.1016/S0143-7208(98)00076-X.

[37] Cockett KRF, Rattee ID, Stevens CB. Some observations on the effect of urea on the dyeing behaviour of wool at low temperatures. J Soc Dye Colour 1969;85:461–8. https://doi.org/10.1111/j.1478-4408.1969.tb02853.x.

[38] Asquith RS, Kwok WF, Otterburn MS. The interaction of urea, thiourea and ammonium thiocyanate with dyes in solution in cold dyeing systems. J Soc Dye Colour 1979;95:20–3. https://doi.org/https://doi.org/10.1111/j.1478-4408.1979.tb03431.x.

[39] Valko EI. Textile auxiliaries in dyeing. Rev Prog Color Relat Top 1972;3:50–62. https://doi.org/10.1111/j.1478-4408.1972.tb00191.x.

[40] Rabinowitch E, Epstein LF. Polymerization of dyestuffs in solution. Thionine and methylene blue. J Am Chem Soc 1941;63:69–78. https://doi.org/10.1021/ja01846a011.

[41] Lemin DR, Vickerstaff T. The aggregation of direct dyes and of methylene blue 2B in aqueous solution. Trans Faraday Soc 1947;43:491–502. https://doi.org/10.1039/tf9474300491.

[42] Yatome C, Ogawa T, Takase Y. The effect of urea, formamide and their derivatives on the aggregation of basic dyes (xanthene dyes). Sen'i Gakkaishi 1973;29:T556–63. https://doi.org/10.2115/fiber.29.12_T556.

[43] Nuñez SC, Yoshimura TM, Ribeiro MS, Junqueira HC, Maciel C, Coutinho-Neto MD, et al. Urea enhances the photodynamic efficiency of methylene blue. J Photochem Photobiol B Biol 2015;150:31–7. https://doi.org/10.1016/j.jphotobiol.2015.03.018.

[44] Booth JJ, Abbott S, Shimizu S. Mechanism of hydrophobic drug solubilization by small molecule hydrotropes. J Phys Chem B 2012;116:14915–21. https://doi.org/10.1021/jp309819r.

[45] Booth JJ, Omar M, Abbott S, Shimizu S. Hydrotrope accumulation around the drug: the driving force for solubilization and minimum hydrotrope concentration for nicotinamide and urea. Phys Chem Chem Phys 2015;17:8028–37. https://doi.org/10.1039/C4CP05414H.

[46] Abbott S, Booth JJ, Shimizu S. Practical molecular thermodynamics for greener solution chemistry. Green Chem 2017;19:68–75. https://doi.org/10.1039/C6GC03002E.

[47] Coffman RE, Kildsig DO. Hydrotropic solubilization - Mechanistic studies. Pharm Res 1996;13:1460–3. https://doi.org/10.1023/A:1016011125302.

[48] Mukerjee P, Ray A. The effect of urea on micelle formation and hydrophobic bonding. J Phys Chem 1963;67:190–2. https://doi.org/10.1021/j100795a046.

[49] Katayama A, Matsuura T, Konishi K, Kuroki N. Effect of urea on the aqueous solubility of dispersed dyes. Kolloid-Z Z Polym 1964;202:157–61.

[50] Sanghvi R, Evans D, Yalkowsky SH. Stacking complexation by nicotinamide: A useful way of enhancing drug solubility. Int J Pharm 2007;336:35–41. https://doi.org/10.1016/j.ijpharm.2006.11.025.

[51] Cui Y. Parallel stacking of caffeine with riboflavin in aqueous solutions: The potential mechanism for hydrotropic solubilization of riboflavin. Int J Pharm 2010;397:36–43. https://doi.org/10.1016/j.ijpharm.2010.06.043.

[52] Alexander P, Stacey KA. Effect of organic solvents on wool dyeing. J Soc Dye Colour 1956;72:241.

[53] Takagishi T, Katayama A, Kuroki N. Effects of tetraalkylammonium halides on the aqueous solubilities of disperse dyes. Sen'i Gakkaishi 1969;25:373–80. https://doi.org/10.2115/fiber.25.373.

[54] Levy M, Magoulas JP. Effect of urea on hydrogen bonding in some dicarboxylic acids. J Am Chem Soc 1962;84:1345–9. https://doi.org/10.1021/ja00867a003.

[55] Shimizu S, Booth JJ, Abbott S. Hydrotropy: binding models vs. statistical thermodynamics. Phys Chem Chem Phys 2013;15:20625–32. https://doi.org/10.1039/c3cp53791a.

[56] Shimizu S, Matubayasi N. Hydrotropy: Monomer-micelle equilibrium and minimum hydrotrope concentration. J Phys Chem B 2014;118:10515–24. https://doi.org/10.1021/jp505869m.

[57] Shimizu S, Matubayasi N. The origin of cooperative solubilisation by hydrotropes. Phys Chem Chem Phys 2016;18:25621–8. https://doi.org/10.1039/C6CP04823D.

[58] Shimizu S, Matubayasi N. Unifying hydrotropy under Gibbs phase rule. Phys Chem Chem Phys 2017;19:23597–605. https://doi.org/10.1039/c7cp02132a.

[59] Shimizu S. Estimating hydration changes upon biomolecular reactions from osmotic stress, high pressure, and preferential hydration experiments. Proc Natl Acad Sci 2004;101:1195–9. https://doi.org/10.1073/pnas.0305836101.

[60] Shimizu S, Matubayasi N. Preferential solvation: Dividing surface vs excess numbers. J Phys Chem B 2014;118:3922–30. https://doi.org/10.1021/jp410567c.

[61] Reid JESJ, Aquino PHG, Walker AJ, Karadakov PB, Shimizu S. Statistical thermodynamics unveils how ions influence an aqueous Diels-Alder reaction. ChemPhysChem

2019;20:1538–44. https://doi.org/10.1002/cphc.201900024.

[62] Chalikian T V. Volumetric properties of proteins. Annu Rev Biophys Biomol Struct 2003;32:207–35. https://doi.org/10.1146/annurev.biophys.32.110601.141709.

[63] Shimizu S. Caffeine dimerization: effects of sugar, salts, and water structure. Food Funct 2015;6:3228–35. https://doi.org/10.1039/C5FO00610D.

[64] Stokes R. Osmotic coefficients of concentrated aqueous urea solutions from freezing-point measurements. J Phys Chem 1966;70:1199–203. https://doi.org/10.1021/j100876a038.

[65] Kawahara K, Tanford C. Viscosity and density of aqueous solutions of urea and guanidine hydrochloride. J Biol Chem 1966;241:3228–32. https://doi.org/10.1016/s0021-9258(18)96519-1.

[66] Lepori L, Gianni P. Partial molar volumes of ionic and nonionic organic solutes in water: A simple additivity scheme based on the intrinsic volume approach. J Solution Chem 2000;29:405–47. https://doi.org/10.1023/A:1005150616038.

[67] Frisch MJ., Trucks GW., Schlegel HB., Scuseria GE., Robb MA., Cheeseman JR., et al. Gaussian 09, Revision A.02 2016.

[68] Connolly ML. Analytical molecular surface calculation. J Appl Crystallogr 1983;16:548–58. https://doi.org/10.1107/S0021889883010985.

[69] Ohling W. The effect of pressure on the self-association of dyes in aqueous solutions studied by cable temperature-jump relaxation spectroscopy. Berichte Bunsengesell Phys Chem 1984;88:109–15. https://doi.org/10.1002/bbpc.19840880207.

[70] Roberts ER, Drickamer HG. High-pressure study of rhodamine B in solution and adsorbed on oriented single-crystal ZnO. J Phys Chem 1985;89:3092–5. https://doi.org/10.1021/j100260a028.

[71] Shimizu S. Formulating rationally via statistical thermodynamics. Curr Opin Colloid Interface Sci 2020;48:53–64. https://doi.org/10.1016/j.cocis.2020.03.008.

[72] Hansen CM. Hansen Solubility Parameters : A User's Handbook. Boca Raton, FL: CRC Press; 2007. https://doi.org/10.1201/9781420006834.

[73] Klamt A. Conductor-like screening model for real solvents: A new approach to the quantitative calculation of solvation phenomena. J Phys Chem 1995;99:2224–35. https://doi.org/10.1021/j100007a062.

[74] Abbott S, Shimizu S. Green solubility for coatings and adhesives. RSC Green Chem., Royal Society of Chemistry; 2019, p. 18–48. https://doi.org/10.1039/9781788012997-00018.

[75] Naleem N, Bentenitis N, Smith PE. A Kirkwood-Buff derived force field for alkaline earth halide salts. J Chem Phys 2018;148. https://doi.org/10.1063/1.5019454.

[76] Hölzl C, Kibies P, Imoto S, Frach R, Suladze S, Winter R, et al. Design principles for high-pressure force fields: Aqueous TMAO solutions from ambient to kilobar pressures. J Chem Phys 2016;144:144104. https://doi.org/10.1063/1.4944991.

[77] Shimizu S, Matubayasi N. Cooperativity in micellar solubilization. Phys Chem Chem Phys 2021;23:8705–16. https://doi.org/10.1039/D0CP06479C.

[78] Shimizu S, Abbott S. How entrainers enhance solubility in supercritical carbon dioxide. J Phys Chem B 2016;120:3713–23. https://doi.org/10.1021/acs.jpcb.6b01380.

[79] Abbott S, Shimizu S. Understanding entrainer effects in supercritical CO2. RSC Green Chem., 2018, p. 14–39. https://doi.org/10.1039/9781788013543-00014.

[80] Abranches DO, Benfica J, Soares BP, Leal-Duaso A, Sintra TE, Pires E, et al. Unveiling the mechanism of hydrotropy: Evidence for water-mediated aggregation of hydrotropes around the solute. Chem Commun 2020;56:7143–6. https://doi.org/10.1039/d0cc03217d.

Tables

Table 1: Structural formulae and numbering of the dyes used for dye solubilization study.

no.	dye	Chemical structure of dye
I	Azobenzene	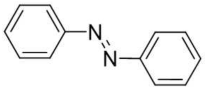
II	Biphenyl	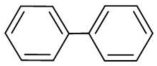
III	4-Aminoazobenzene	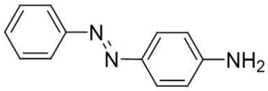
IV	Methyl Yellow	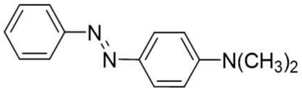
V	N,N-di(2-hydroxyethyl)-4-	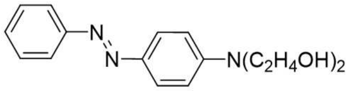
VI	Naphthyl Red	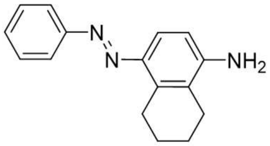
VII	Solvent Yellow 7	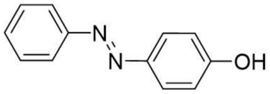

Table 2: Fitting parameters for Figure 2. The functions used to fit the experimental data were $y = ax^2 + bx + c$, where $x = RT \ln a_1$.

dye	a	b
I	-20.9	14.1
II	-25.8	16.0
III	-30.1	17.5
IV	-48.7	23.3
V	-61.6	25.2
VI	-118.0	39.3
VII	-29.0	18.6

Table 3: Values of the partial molar volume (V_u) , excluded volume (V_E), and their differences for each dye (see Table 1).

dye	V_u / cm^3 · mol^{-1}	V_E / cm^3 · mol^{-1}	V_u' / cm^3 · mol^{-1}
I	160.5	181.8	-21.2
II	137.3	161.0	-23.7
III	172.0	193.3	-21.3
IV	208.7	226.7	-18.0
V	240.3	280.1	-39.8
VI	214.2	240.3	-26.1
VII	168.3	191.1	-22.8

Table 4: Structural formulae and numbering of the dyes used for dye dimerization study.

no.	dye	Chemical structure of dye
VIII	Methylene Blue	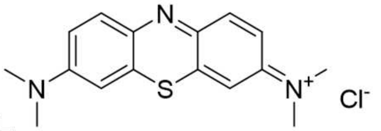
IX	Rhodamine B	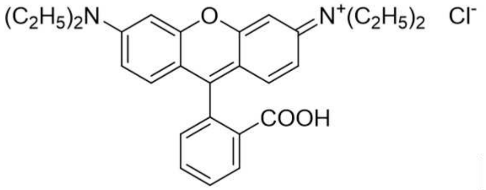

Table 5: Comparison of the values of the first and second terms in the right-hand side of equation (12).

dye	$V_1\left(\frac{\partial \ln K_a}{\partial \ln a_1}\right)$	$-\Delta V_u$ ($\mathrm{cm^3\ mol^{-1}}$)
VIII	1077.6	8.3
IX	1234.4	4.2